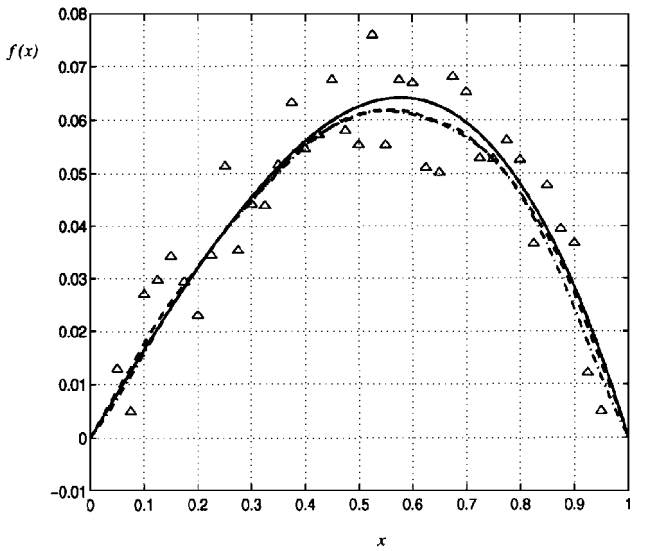

Fig. 2 Interpolation of data with noise for optimal α: ——, $F(x)$; – – –, $\tilde{f}(x)$; and –·–, $f_a(x)$.

Use of Eq. (20) requires a priori knowledge regarding the intensity of the random noise in measurements. This is usually available in engineering applications. The optimal α, which acts as a Lagrange multiplier, was determined through the dichotomous search technique.[7] The regularized curve of Fig. 2 (– – –) shows that the developed method of data analysis can successfully discriminate between noise and the physical system response.

B. Results from Numerical Approximation

The numerical approximation by basis expansion consisted of seven ($M = 7$) Gaussian radial basis functions in which the transfer function centers were uniformly distributed in the segment [0, 1] with the center of the two boundary functions located at $x = 0$ and 1, respectively. The parameters Δ_k of Eq. (14), describing the localization properties of the Gaussian function, were all selected to be equal to $\frac{1}{6}$. Figure 1 illustrates the acceptable matching between the analytical solution of the regularization problem and the numerical approximation. Figure 2 shows that the performance of the basis expansion in modeling with the noisy data of Sec. III.A is satisfactory. In the interpolation study, α was determined such that Eqs. (16) and (17) were satisfied with Eq. (19) for $f = f_a$.

IV. Summary

A method of combining experimental data and physical models is presented. Specifically, physical models of engineering interest can be expressed in the form of empirical, differential, and/or integral equations of varying degrees of fidelity. These model equations can be incorporated in the form of a regularizing functional for a robust matching of experimental data. The method can be viewed as the adjustment of a low-fidelity, and computationally inexpensive, mathematical model response by experimental data. The developed method also can be viewed as an efficient procedure for interpolating experimental data by utilizing physically motivated criteria. Further, it has been shown how the developed method can be used to successfully extrapolate the physical system response at unmeasured coordinates and filter noisy experimental measurements. The radial basis expansion has been examined as the computational apparatus of the developed method. However, the developments of the paper retain a sufficient level of generality and can be implemented in conjunction with any of the commonly used methods, including finite difference and conventional finite elements.

Acknowledgment

This work was supported under Office of Naval Research Grant N00014-95-1-0741.

References

[1]Doebelin, E. O., *Engineering Experimentation: Planning, Execution, Reporting*, McGraw–Hill, New York, 1995.

[2]Tikhonov, A. N., and Arsenin, V. Y., *Solution of Ill-Posed Problems*, Winston, Washington, DC, 1977.

[3]Poggio, T., and Girosi, F., "Networks for Approximation and Learning," *Proceedings of the IEEE*, Vol. 78, No. 9, 1990, pp. 1481–1497.

[4]Girosi, F., Jones, M., and Poggio, T., "Regularization Theory and Neural Network Architectures," *Neural Computation*, Vol. 7, No. 2, 1995, pp. 219–269.

[5]Bishop, C. M., "Curvature-Driven Smoothing: A Learning Algorithm for Feedforward Networks," *IEEE Transactions on Neural Networks*, Vol. 4, No. 5, 1993, pp. 882–884.

[6]Fletcher, C. A. J., *Computational Galerkin Methods*, Springer–Verlag, New York, 1984.

[7]Stoecker, W. F., *Design of Thermal Systems*, McGraw–Hill, New York, 1989, pp. 189, 190.

P. R. Bandyopadhyay
Associate Editor

Application of Dual Sorption Theory to Pressure-Sensitive Paints

J. P. Hubner* and B. F. Carroll†
University of Florida, Gainesville, Florida 32611-6250

Introduction

THIS Note describes the application of a nonlinear dual sorption theory[1,2] for modeling the steady-state emission of pressure-sensitive paints (PSPs). Calibration comparisons with polynomial expansion models are presented over a 1-atm pressure range for two PSP formulations.

Theoretical Background

PSPs are composed of probe molecules—luminophors—doped into an oxygen permeable binder and dissolved in a thinning agent that forms a coating when sprayed onto a surface of interest. The luminescent intensity variation of most PSPs used in aerodynamic applications is described by the Stern–Volmer relation[3–5]

$$I_0/I = 1 + K[O_2] \tag{1}$$

where I_0 is the unquenched intensity, I is the quenched intensity, K is the Stern–Volmer coefficient, and $[O_2]$ is the oxygen concentration within the coating. The concentration of sorbed oxygen in a liquid is related to the partial pressure of oxygen by Henry's law:

$$[O_2] = \sigma(T)\,P_{O_2} \tag{2a}$$

where

$$P_{O_2} = \chi_{O_2} P \tag{2b}$$

and where σ is the solubility coefficient (modeled as a function of temperature only), P is pressure, T is temperature, and χ is the mole fraction of the penetrant. When ratioing intensities at two pressure levels, one designated as a reference (ref), the common form[3–6] of the intensity–pressure relationship for PSPs is derived from Eqs. (1) and (2a):

$$(I_{ref}/I) = A + B(P/P_{ref}) \tag{3}$$

where the coating sensitivities A and B are functions of temperature and reference conditions if all other conditions are held constant, e.g., illumination intensity.

Received April 13, 1997; revision received July 25, 1997; accepted for publication July 25, 1997.

*Postdoctoral Associate, Department of Aerospace Engineering, Mechanics, and Engineering Science, P.O. Box 116250. Member AIAA.

†Associate Professor, Department of Aerospace Engineering, Mechanics, and Engineering Science, P.O. Box 116250. Member AIAA.

For many aerodynamic applications, the first-order polynomial relationship of Eq. (3) is assumed, providing an adequate calibration over a limited pressure range of interest. Often, over expanded pressure ranges (0–1 atm), the intensity response is not well described by Eq. (3), indicating that the solubility coefficient is a function of pressure and temperature,

$$[O_2] = \sigma\left(T,\, P_{O_2}\right) P_{O_2} \tag{4}$$

In such cases the intensity–pressure calibration is generally approximated by a higher-order polynomial expansion[3,4,6]:

$$(I_{\text{ref}}/I) = A + B(P/P_{\text{ref}}) + C(P/P_{\text{ref}})^2 + \cdots \tag{5}$$

While convenient, polynomial calibrations do not always accurately model the intensity–pressure relationship over large pressure ranges, leading to poor predictions at extrapolated intensities. Dissolving luminophors within a polymer film creates a heterogeneous environment on a microscopic scale, especially as the luminophor concentration within the binder is increased. The luminescent probes can become unevenly dispersed, and molecular aggregation can occur, leading to self-quenching of excited probes and multiple exponential decays (as opposed to single exponential decays for dyes in a dilute fluid solvent—a homogeneous environment).[7,8] At lower levels of penetrant concentration (lower pressures), the longer-rate decays are less likely to be quenched, providing additional contribution to the overall PSP luminescence. This is an effect similar to preferential sorption and penetrant immobilization, which is present in many inhomogeneous polymer films.

To more accurately model the intensity–pressure calibration of PSPs, an alternative sorption and quenching process is applied based on dual sorption theory.[1,2] This nonlinear model has been used extensively over the past few decades in a diverse number of phenomena, including gas sorption and diffusion in composite or heterogeneous media. The penetrant concentration, Eq. (6), is composed of a linear term (l) representing the limiting case of normal Henry's law sorption and a nonlinear term (nl) representing Langmuir's model of penetrant immobilization:

$$[O_2] = [O_2]_l + [O_2]_{\text{nl}} = \sigma_l(T) P_{O_2} + \sigma_{\text{nl}}(T) \frac{b(T) P_{O_2}}{1 + b(T) P_{O_2}} \tag{6}$$

where b is the affinity coefficient (a ratio of absorption to desorption of penetrant). As the value of $b P_{O_2}$ is increased in Eq. (6), the immobilized oxygen concentration reaches a limit of σ_{nl}, and the sorption follows Henry's law plus a constant,

$$[O_2] = \sigma_l P_{O_2} + \sigma_{\text{nl}} \tag{7}$$

In terms of the change of oxygen concentration with partial pressure, two limiting regions of sorption exist: a low-pressure state,

$$\lim_{P_{O_2} \to 0} \frac{\partial [O_2]}{\partial P_{O_2}} = \sigma_l + \sigma_{\text{nl}} b \tag{8a}$$

and a high-pressure state,

$$\lim_{P_{O_2} \to \infty} \frac{\partial [O_2]}{\partial P_{O_2}} = \sigma_l \tag{8b}$$

Applying the dual sorption model to Eq. (1) results in a functional form of the intensity–pressure relationship as follows:

$$\frac{I_{\text{ref}}}{I} = A + B\frac{P}{P_{\text{ref}}} + C\frac{D(P/P_{\text{ref}})}{1 + D(P/P_{\text{ref}})} \tag{9}$$

Again, the coating sensitivities (A, B, C, and D) are a function of temperature and reference conditions. Rewriting Eq. (9) results in a quadratic that can be used to form an explicit expression of pressure as a function of intensity:

$$\alpha(P/P_{\text{ref}})^2 + \beta(P/P_{\text{ref}}) + \gamma = 0 \tag{10}$$

where

$$\alpha = BD, \qquad \beta = [A + C - (I_{\text{ref}}/I)]D + B, \qquad \gamma = A - (I_{\text{ref}}/I)$$

Experimental Results and Discussion

Previous laboratory results were analyzed for two PSP samples: a tris-(4,7-diphenylphenanthroline)-Ru(II) dichloride probe in a polydimethylsiloxane binder (PSP-A)[8] and a Pt(II) tetra(pentafluorophenyl) porphyrin probe in a fine powder silica gel binder (PSP-B). Both of these probe molecules were chosen for their suitable aerodynamic testing characteristics. Each sample was installed in an environmental chamber, and emission intensities were measured using a cooled, 14-bit charge-coupled device camera. The pressure was varied over a range from 0.05–1.0 atm, the latter being the reference state. Appropriate bandpass filtering of the excitation (450 nm) and emission (650 nm) was performed.

Figure 1 is an intensity–pressure plot of the PSP-A raw data along an isotherm ($T = 25°C$). Applied to a sample set of the data (the 10 lower pressure data points, designated by the closed square symbols) were first- through third-order polynomials and the dual sorption (DS) fit. A least-squares regression technique was employed in each case, the latter using the Levenburg–Marquardt iterative algorithm for nonlinear equations. As shown in Fig. 1, the inverse of intensity vs pressure does not scale linearly over the measured pressure range. Table 1 lists the coefficients for the data fits and quantifies the rms error for both the inclusive set (closed square symbols) and exclusive set (open square symbols) of data. The latter gives a quantifiable indication of the predictive ability of each calibration. Clearly, the dual sorption model best fits the data, showing the lowest associated errors. The second- and third-order polynomials spuriously fit the inclusive data, providing a useful interpolation tool; however, both deviate when extrapolating beyond the data range. At pressure ratios greater than 1, the quadratic model erroneously predicts an increase in intensity with pressure (a decrease in I_{ref}/I), and the third-order fit exaggerates the intensity decrease with pressure due to an inflection point at $P/P_{\text{ref}} = 0.63$. Similar results are shown in Fig. 2 for the PSP-B data.

Because Eq. (9) is nonlinear, an iterative technique was used to solve calibration coefficients for a specified tolerance of the correlation coefficient. At least 8–10 data points were sufficient for the calibration coefficients to converge in relatively few iterations (10–20) despite adjustments in the initial seed coefficient values. When only six data points were employed, however, minor adjustments in

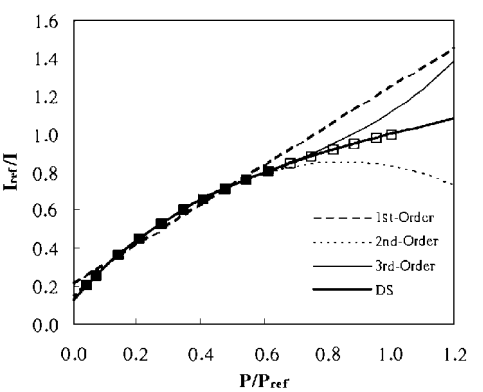

Fig. 1 Intensity vs pressure calibration for PSP-A.

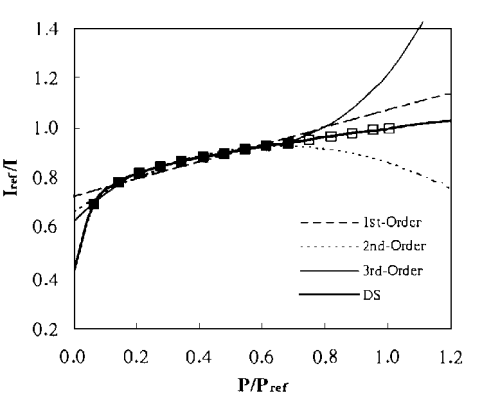

Fig. 2 Intensity vs pressure calibration for PSP-B.

Table 1 Calibration coefficients and error measurements for the two PSP formulations

	PSP-A				PSP-B			
	1st	2nd	3rd	DS[a]	1st	2nd	3rd	DS[a]
Coefficient								
A	0.21	0.15	0.13	0.13	0.73	0.67	0.62	0.42
B	1.04	1.66	1.93	0.16	0.35	0.79	1.38	0.16
C	——	−0.97	−2.01	1.13	——	−0.59	−2.51	0.43
D	——	——	1.06	1.71	——	——	1.73	24.2
rmse[b]								
(inclusive)	0.0332	0.0058	0.0011	0.0004	0.0256	0.0131	0.0059	0.0002
(exclusive)	0.1038	0.0323	0.0110	0.0010	0.0447	0.0754	0.1225	0.0013

[a]DS = dual sorption. [b]rmse = root mean square error.

the initial seed values led to differences in the resulting calibration coefficients. To ensure a well-balanced calibration over a large pressure range (>1 atm), an equal number of measurements in the linear and nonlinear regions of the curve is suggested. The pressure value separating these two regions can be determined using Eq. (11):

$$B\frac{(1+DP_{\text{ratio}})^2}{CD}=1 \tag{11}$$

where $P_{\text{ratio}} = P/P_{\text{ref}}$. Using the calibration coefficients listed in Table 1, pressure ratios of 1.45 and 0.29 are calculated for PSP-A and PSP-B, respectively. Thus, additional measurements at higher pressure ratios for PSP-A and lower pressure ratios for PSP-B would further decrease the uncertainty in the corresponding calibration coefficients of those regions.

Conclusions

The application of dual sorption theory to the calibration of PSPs is presented. The nonlinear model better represents the steady-state sorption and quenching processes within the PSP coatings and yields a superior intensity–pressure calibration when applied over broad pressure ranges, in extrapolated regions, or to coatings with high luminophor loading. The tradeoff is the model's inherent nonlinearity, which requires an iterating technique for determining the calibration coefficients and leads to complications when decoupling the temperature sensitivity.[9] For high pressures and limited ranges, a second-order polynomial or linear model will suffice.

References

[1]Vieth, W. R., Howell, J. M., and Hsieh, J. H., "Dual Sorption Theory," *Journal of Membrane Science*, Vol. 1, 1976, pp. 177–220.

[2]Rogers, C. E., "Permeation of Gases and Vapours in Polymers," *Polymer Permeability*, edited by J. Comyn, Elsevier, Amsterdam, 1985, pp. 11–73.

[3]Lui, T., Campbell, B. T., Burns, S. P., and Sullivan, J. P., "Temperature- and Pressure-Sensitive Luminescent Paints in Aerodynamics," *Applied Mechanics Review*, Vol. 50, No. 4, 1997, pp. 227–246.

[4]McLachlan, B. G., and Bell, J. H., "Pressure-Sensitive Paint in Aerodynamic Testing," *Experimental Thermal and Fluid Sciences*, Vol. 10, No. 4, 1995, pp. 470–485.

[5]Morris, M. J., Donovan, J. F., Kegelmman, J. T., Schwab, S. D., Levy, R. L., and Crites, R. C., "Aerodynamic Applications of Pressure Sensitive Paint," *AIAA Journal*, Vol. 31, No. 3, 1993, pp. 419–425.

[6]Vollan, A., and Alati, L., "A New Optical Pressure Measurement System (OPMS)," *Proceedings of the 14th International Congress on Instrumentation in Aerospace Simulation Facilities*, Inst. of Electrical and Electronics Engineers, New York, 1991, pp. 10–16.

[7]James, D. R., Lui, Y.-S., Demayo, P., and Ware, W. R., "Distributions of Fluorescence Lifetimes: Consequences for the Photophysics of Molecules Absorbed on Surfaces," *Chemical Physics Letters*, Vol. 20, No. 4/5, 1985, pp. 460–465.

[8]Schanze, K. S., Carroll, B. F., Korotkevitch, S., and Morris, M., "Concerning the Temperature Dependence of Pressure Sensitive Paint," *AIAA Journal*, Vol. 35, No. 2, 1997, pp. 306–310.

[9]Hubner, J. P., Carroll, B. F., and Schanze, K. S., "Temperature Compensation Model for Pressure-Sensitive Paint," *Proceedings of the 1997 ASME Fluids Engineering Division Summer Meeting* (CD-ROM), American Society of Mechanical Engineers, New York, 1997, pp. 1–6 (Paper 3470).

G. Laufer
Associate Editor

Nonaxisymmetric Exact Piezothermoelastic Solution for Laminated Cylindrical Shell

Santosh Kapuria*
Engineers India Ltd., New Delhi 110066, India
P. C. Dumir†
Indian Institute of Technology, New Delhi 110066, India
and
S. Sengupta‡
Engineers India Ltd., New Delhi 110066, India

I. Introduction

THE electroelastic coupling in piezoelectric materials is used for active control of smart structures. Two-dimensional solutions have been presented for the thermoelectroelastic response of hybrid plates and shells, using classical and first-order shear deformation theories.[1–3] Few three-dimensional piezothermoelastic solutions are available for hybrid finite plates and shells.[4–6] These are needed to assess two-dimensional theories. Xu and Noor[6] presented three-dimensional solution for a simply supported finite cylindrical hybrid shell but did not include the case of potential difference applied across a piezoelectric layer. We present a three-dimensional solution for such a case. The governing differential equations with variable coefficients are solved by the modified Frobenius method. The constants in the general solution and the extraneous charge densities at the interfaces where potential or potential difference is prescribed are determined from the boundary and interface conditions. Results are presented to illustrate the effect of the length parameter.

II. General Solution of Governing Equations

Consider a finite circular cylindrical hybrid shell of mean radius R, thickness h, and length a, having L orthotropic layers with their principal directions along the radial, circumferential, and axial direction. The inner and outer radii are R_i, $R_o = R \mp h/2$. The innermost layer is named as the first layer. The interface between the kth and the $(k+1)$th layer is named as the kth interface. Let the thickness of the kth layer be $t^{(k)}$ and its inner radius be $R_1^{(k)}$. The layer superscript is omitted unless needed for clarity. The ends of the shell are electrically grounded, maintained at stress-free temperature, and simply supported to allow only the displacement normal to the boundary. Let u, v, w be the displacements; σ_r, σ_θ, σ_z, $\tau_{\theta z}$, τ_{zr}, $\tau_{r\theta}$ the stresses;

Received Feb. 6, 1996; revision received Nov. 10, 1996; accepted for publication July 24, 1997.

*Senior Engineer, Engineering and Technology Development (Analysis), Bhikaijee Kama Place.

†Professor, Applied Mechanics Department.

‡Chief Consultant, Engineering and Technology Development (Analysis), Bhikaijee Kama Place.